



Discovery of X-Ray Polarization from the Black Hole Transient Swift J1727.8–1613

Alexandra Veledina^{1,2} , Fabio Muleri³ , Michal Dovčiak⁴ , Juri Poutanen¹ , Ajay Ratheesh³ , Fiamma Capitanio³ ,
 Giorgio Matt⁵ , Paolo Soffitta³ , Allyn F. Tennant⁶ , Michela Negro⁷ , Philip Kaaret⁶ , Enrico Costa³ , Adam Ingram⁸ ,
 Jiří Svoboda⁴ , Henric Krawczynski⁹ , Stefano Bianchi⁵ , James F. Steiner¹⁰ , Javier A. García¹¹ , Vadim Kravtsov¹ ,
 Anagha P. Nitindala¹ , Melissa Ewing⁸ , Guglielmo Mastroserio¹² , Andrea Marinucci¹³ , Francesco Ursini⁵ ,
 Francesco Tombesi^{14,15,16} , Sergey S. Tsygankov¹ , Yi-Jung Yang^{17,18} , Martin C. Weisskopf⁶ , Sergei A. Trushkin¹⁹ ,
 Elise Egron¹² , Maria Noemi Iacolina²⁰ , Maura Pilia¹² , Lorenzo Marra⁵ , Romana Mikušincová⁵ , Edward Nathan²¹ ,
 Maxime Para^{5,22} , Pierre-Olivier Petrucci²² , Jakub Podgorný^{4,23,24} , Stefano Tugliani^{25,26} , Silvia Zane²⁷ ,
 Wenda Zhang²⁸ , Iván Agudo²⁹ , Lucio A. Antonelli^{30,31} , Matteo Bachetti¹² , Luca Baldini^{32,33} ,
 Wayne H. Baumgartner⁶ , Ronaldo Bellazzini³² , Stephen D. Bongiorno⁶ , Raffaella Bonino^{25,26} , Alessandro Brez³² ,
 Niccolò Bucciantini^{34,35,36} , Simone Castellano³² , Elisabetta Cavazzuti¹³ , Chien-Ting Chen³⁷ , Stefano Ciprini^{15,31} ,
 Alessandra De Rosa³ , Ettore Del Monte³ , Laura Di Gesu¹³ , Niccolò Di Lalla³⁸ , Alessandro Di Marco³ ,
 Immacolata Donnarumma¹³ , Victor Doroshenko³⁹ , Steven R. Ehlert⁶ , Teruaki Enoto⁴⁰ , Yuri Evangelista³ ,
 Sergio Fabiani³ , Riccardo Ferrazzoli³ , Shuichi Gunji⁴¹ , Kiyoshi Hayashida^{42,57} , Jeremy Heyl⁴³ , Wataru Iwakiri⁴⁴ ,
 Svetlana G. Jorstad^{45,46} , Vladimir Karas⁴ , Fabian Kislak⁴⁷ , Takao Kitaguchi⁴⁰ , Jeffery J. Kolodziejczak⁶ ,
 Fabio La Monaca³ , Luca Latronico²⁵ , Ioannis Liodakis⁶ , Simone Maldera²⁵ , Alberto Manfreda⁴⁸ , Frédéric Marin²³ ,
 Alan P. Marscher⁴⁵ , Herman L. Marshall⁴⁹ , Francesco Massaro^{25,26} , Ikuyuki Mitsuishi⁵⁰ , Tsunefumi Mizuno⁵¹ ,
 Chi-Yung Ng¹⁷ , Stephen L. O'Dell⁶ , Nicola Omodei³⁸ , Chiara Oppedisano²⁵ , Alessandro Papitto³⁰ ,
 George G. Pavlov⁵² , Abel L. Peirson³⁸ , Matteo Perri^{30,31} , Melissa Pesce-Rollins³² , Andrea Possenti¹² ,
 Simonetta Puccetti³¹ , Brian D. Ramsey⁶ , John Rankin³ , Oliver J. Roberts³⁷ , Roger W. Romani³⁸ , Carmelo Sgrò³² ,
 Patrick Slane¹⁰ , Gloria Spandre³² , Douglas A. Swartz³⁷ , Toru Tamagawa⁴⁰ , Fabrizio Tavecchio⁵³ ,
 Roberto Taverna⁵⁴ , Yuzuru Tawara⁵⁰ , Nicholas E. Thomas^{7,15,16} , Alessio Trois¹² , Roberto Turolla^{27,54} , Jacco Vink⁵⁵ ,
 Kinwah Wu²⁷ , and Fei Xie^{3,56}

¹ Department of Physics and Astronomy, FI-20014 University of Turku, Finland

² Nordita, KTH Royal Institute of Technology and Stockholm University, Hannes Alfvéns väg 12, SE-10691 Stockholm, Sweden

³ INAF Istituto di Astrofisica e Planetologia Spaziali, Via del Fosso del Cavaliere 100, I-00133 Roma, Italy

⁴ Astronomical Institute of the Czech Academy of Sciences, Boční II 1401/1, 14100 Praha 4, Czech Republic

⁵ Dipartimento di Matematica e Fisica, Università degli Studi Roma Tre, Via della Vasca Navale 84, I-00146 Roma, Italy

⁶ NASA Marshall Space Flight Center, Huntsville, AL 35812, USA

⁷ Department of Physics and Astronomy, Louisiana State University, Baton Rouge, LA 70803, USA

⁸ School of Mathematics, Statistics, and Physics, Newcastle University, Newcastle upon Tyne NE1 7RU, UK

⁹ Physics Department and McDonnell Center for the Space Sciences, Washington University in St. Louis, St. Louis, MO 63130, USA

¹⁰ Center for Astrophysics, Harvard & Smithsonian, 60 Garden St., Cambridge, MA 02138, USA

¹¹ X-ray Astrophysics Laboratory, NASA Goddard Space Flight Center, Greenbelt, MD 20771, USA

¹² INAF Osservatorio Astronomico di Cagliari, Via della Scienza 5, I-09047 Selargius (CA), Italy

¹³ Agenzia Spaziale Italiana, Via del Politecnico snc, I-00133 Roma, Italy

¹⁴ Dipartimento di Fisica, Università degli Studi di Roma “Tor Vergata,” Via della Ricerca Scientifica 1, I-00133 Roma, Italy

¹⁵ Istituto Nazionale di Fisica Nucleare, Sezione di Roma “Tor Vergata,” Via della Ricerca Scientifica 1, I-00133 Roma, Italy

¹⁶ Department of Astronomy, University of Maryland, College Park, MD 20742, USA

¹⁷ Department of Physics, The University of Hong Kong, Pokfulam Rd., Hong Kong

¹⁸ Laboratory for Space Research, The University of Hong Kong, Cyberport 4, Hong Kong

¹⁹ Special Astrophysical Observatory of the Russian Academy of Sciences, Nizhnij Arkhyz, 369167, Karachayevo-Cherkessia, Russia

²⁰ Agenzia Spaziale Italiana, Via della Scienza 5, I-09047, Selargius (CA), Italy

²¹ Cahill Center for Astronomy and Astrophysics, California Institute of Technology, Pasadena, CA 91125, USA

²² Université Grenoble Alpes, CNRS, IPAG, F-38000 Grenoble, France

²³ Université de Strasbourg, CNRS, Observatoire Astronomique de Strasbourg, UMR 7550, F-67000 Strasbourg, France

²⁴ Astronomical Institute, Charles University, V Holešovičkách 2, CZ-18000, Prague, Czech Republic

²⁵ Istituto Nazionale di Fisica Nucleare, Sezione di Torino, Via Pietro Giuria 1, I-10125, Torino, Italy

²⁶ Dipartimento di Fisica, Università degli Studi di Torino, Via Pietro Giuria 1, I-10125 Torino, Italy

²⁷ Mullard Space Science Laboratory, University College London, Holmbury St Mary, Dorking, Surrey RH5 6NT, UK

²⁸ National Astronomical Observatories, Chinese Academy of Sciences, 20A Datun Rd., Beijing 100101, People’s Republic of China

²⁹ Instituto de Astrofísica de Andalucía—CSIC, Glorieta de la Astronomía s/n, E-18008 Granada, Spain

³⁰ INAF Osservatorio Astronomico di Roma, Via Frascati 33, I-00040 Monte Porzio Catone (RM), Italy

³¹ Space Science Data Center, Agenzia Spaziale Italiana, Via del Politecnico snc, I-00133 Roma, Italy

³² Istituto Nazionale di Fisica Nucleare, Sezione di Pisa, Largo B. Pontecorvo 3, I-56127 Pisa, Italy

³³ Dipartimento di Fisica, Università di Pisa, Largo B. Pontecorvo 3, I-56127 Pisa, Italy

³⁴ INAF Osservatorio Astrofisico di Arcetri, Largo Enrico Fermi 5, I-50125 Firenze, Italy

³⁵ Dipartimento di Fisica e Astronomia, Università degli Studi di Firenze, Via Sansone 1, I-50019 Sesto Fiorentino (FI), Italy

³⁶ Istituto Nazionale di Fisica Nucleare, Sezione di Firenze, Via Sansone 1, I-50019 Sesto Fiorentino (FI), Italy

³⁷ Science and Technology Institute, Universities Space Research Association, Huntsville, AL 35805, USA

³⁸ Department of Physics and Kavli Institute for Particle Astrophysics and Cosmology, Stanford University, Stanford, CA 94305, USA

³⁹ Institut für Astronomie und Astrophysik, Universität Tübingen, Sand 1, D-72076 Tübingen, Germany

⁴⁰ RIKEN Cluster for Pioneering Research, 2-1 Hirosawa, Wako, Saitama 351-0198, Japan

⁴¹ Yamagata University, 1-4-12 Kojirakawa-machi, Yamagata-shi 990-8560, Japan

⁴² Osaka University, 1-1 Yamadaoka, Suita, Osaka 565-0871, Japan

⁴³ University of British Columbia, Vancouver, BC V6T 1Z4, Canada⁴⁴ International Center for Hadron Astrophysics, Chiba University, Chiba 263-8522, Japan⁴⁵ Institute for Astrophysical Research, Boston University, 725 Commonwealth Avenue, Boston, MA 02215, USA⁴⁶ Department of Astrophysics, St. Petersburg State University, Universitetsky pr. 28, Petrodvoretz, 198504 St. Petersburg, Russia⁴⁷ Department of Physics and Astronomy and Space Science Center, University of New Hampshire, Durham, NH 03824, USA⁴⁸ Istituto Nazionale di Fisica Nucleare, Sezione di Napoli, Strada Comunale Cinthia, I-80126 Napoli, Italy⁴⁹ MIT Kavli Institute for Astrophysics and Space Research, Massachusetts Institute of Technology, 77 Massachusetts Avenue, Cambridge, MA 02139, USA⁵⁰ Graduate School of Science, Division of Particle and Astrophysical Science, Nagoya University, Furo-cho, Chikusa-ku, Nagoya, Aichi 464-8602, Japan⁵¹ Hiroshima Astrophysical Science Center, Hiroshima University, 1-3-1 Kagamiyama, Higashi-Hiroshima, Hiroshima 739-8526, Japan⁵² Department of Astronomy and Astrophysics, Pennsylvania State University, University Park, PA 16801, USA⁵³ INAF Osservatorio Astronomico di Brera, Via E. Bianchi 46, I-23807 Merate (LC), Italy⁵⁴ Dipartimento di Fisica e Astronomia, Università degli Studi di Padova, Via Marzolo 8, I-35131 Padova, Italy⁵⁵ Anton Pannekoek Institute for Astronomy & GRAPPA, University of Amsterdam, Science Park 904, 1098 XH Amsterdam, The Netherlands⁵⁶ Guangxi Key Laboratory for Relativistic Astrophysics, School of Physical Science and Technology, Guangxi University, Nanning 530004, People's Republic of China*Received 2023 September 26; revised 2023 October 24; accepted 2023 October 25; published 2023 November 21*

Abstract

We report the first detection of the X-ray polarization of the bright transient Swift J1727.8–1613 with the Imaging X-ray Polarimetry Explorer. The observation was performed at the beginning of the 2023 discovery outburst, when the source resided in the bright hard state. We find a time- and energy-averaged polarization degree of $4.1\% \pm 0.2\%$ and a polarization angle of $2^\circ 2' \pm 1^\circ 3'$ (errors at 68% confidence level; this translates to $\sim 20\sigma$ significance of the polarization detection). This finding suggests that the hot corona emitting the bulk of the detected X-rays is elongated, rather than spherical. The X-ray polarization angle is consistent with that found in submillimeter wavelengths. Since the submillimeter polarization was found to be aligned with the jet direction in other X-ray binaries, this indicates that the corona is elongated orthogonal to the jet.

Unified Astronomy Thesaurus concepts: [Accretion \(14\)](#); [X-ray astronomy \(1810\)](#); [Low-mass x-ray binary stars \(939\)](#); [Polarimetry \(1278\)](#); [Astrophysical black holes \(98\)](#)

1. Introduction

Mass accretion is a fundamental process of energy extraction that powers some of the brightest X-ray sources. It operates very efficiently for compact objects, neutron stars and black holes (BHs), which accrete matter from a nearby companion star. BH X-ray binaries display two major spectral states, hard and soft, which are thought to be linked to different accretion regimes (Zdziarski & Gierliński 2004; Remillard & McClintock 2006; Done et al. 2007). In the soft state, the X-ray spectrum is dominated by a blackbody-like emission that is believed to be produced by a geometrically thin, optically thick accretion disk (Novikov & Thorne 1973; Shakura & Sunyaev 1973; Page & Thorne 1974). In the hard state, the spectrum constitutes a power-law-like continuum, that is generally attributed to Comptonization in a medium with hot electrons (a corona). At the transitions between the canonical states, the hard-intermediate and soft-intermediate, as well as very high (or steep power-law) states have been identified (Homan & Belloni 2005; Belloni 2010).

Transitions of BH X-ray binaries between various spectral states follow a well-known pattern; however, our understanding of the accretion geometry and physical mechanisms producing broadband emission in these states is still incomplete. The geometry and location of the hot medium in the hard spectral state is still a matter of debate (Poutanen et al. 2018; Bambi et al. 2021). The structure of the accretion disk is unclear; its stability in the soft state is puzzling (Dexter &

Quataert 2012; Jiang et al. 2013). Furthermore, the conditions for the source to show the very high state are unknown (Done et al. 2007). X-ray polarimetry is a new diagnostic that may help resolve questions regarding the geometry of the emission region left unanswered by the conventional tools of spectroscopy and timing.

The Imaging X-ray Polarimetry Explorer (IXPE; Weisskopf et al. 2022) provided the first significant detection of 2–8 keV X-ray polarization in the archetypical BH Cyg X-1 (Krawczynski et al. 2022)—the source that originally gave rise to the spectral classifications (Tananbaum et al. 1972). The hot Comptonizing medium visible in the hard spectral state of the binary appeared to be elongated in the plane of the accretion disk. The polarization angle (PA) of X-ray emission was found to be consistent with the position angle of the extended radio source (Miller-Jones et al. 2021), thus confirming, for the first time, that the radio jets are launched along the axis of the (inner) accretion disk. The polarization degree (PD) of $4.0\% \pm 0.2\%$ was higher than expected for the orbital inclination of the source $i \approx 30^\circ$ (Miller-Jones et al. 2021). This can be explained by the inner disk being more highly inclined than the outer disk (Krawczynski et al. 2022) or by an outflow of the hot medium (Poutanen et al. 2023).

The BH X-ray binary Cyg X-3 became the second hard-state target of IXPE. Similarly to Cyg X-1, the source swings between different spectral states, which might be attributed to the same configurations of accreting matter as in Cyg X-1. Contrary to early expectations, a high PD = $20.6\% \pm 0.3\%$ was detected in the hard state (Veledina et al. 2023). The X-ray PA was found to be shifted by 90° with respect to the position angle of the discrete radio ejections, as well as to the submillimeter polarization direction. These unique polarization properties can be explained in terms of a pure reflection scenario. The X-ray polarization observations revealed the

⁵⁷ Deceased.

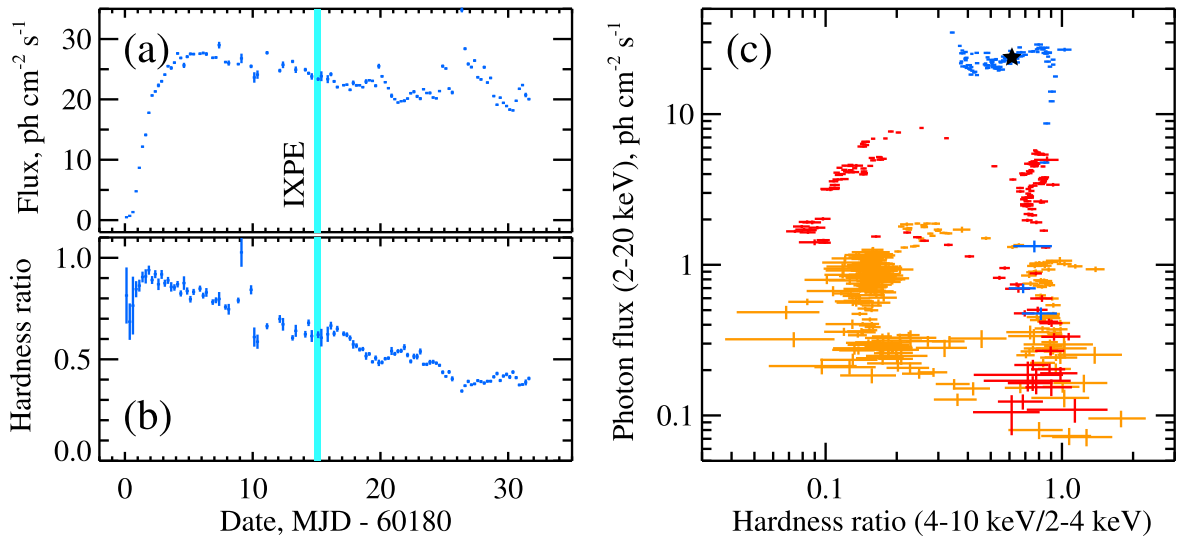


Figure 1. Evolution of Swift J1727.8–1613 during the outburst. (a) MAXI light curve in the 2–20 keV range. The time of the IXPE observation is marked by the cyan vertical line. (b) Hardness ratio, i.e., the ratio of the photon flux in the 4–10 keV band to that in the 2–4 keV band. (c) Hardness–flux diagram. Blue crosses show the evolution of Swift J1727.8–1613 during the current outburst. The position of the source on the diagram during IXPE observation is marked with a black star. For comparison, we also plot the time evolution of MAXI J1820+070 during its 2018 outburst with red crosses and GX 339–4 during its 2010 outburst with the orange crosses. The diagram (c) shows that Swift J1727.8–1613 was observed in the hard state soon after the turning point.

presence of an obscuring and reflecting envelope at high elevation above the disk plane, suggesting this well-studied binary is a Galactic ultraluminous X-ray source.

The aforementioned hard-state sources belong to the class of high-mass X-ray binaries, where the compact object captures matter from the wind of their massive companion. The innermost accretion geometry of low-mass X-ray binary BHs, where the disk forms via Roche lobe overflow, was not yet studied polarimetrically. In this paper, we report on the first X-ray polarization measurement of the Galactic X-ray binary Swift J1727.8–1613.

2. Discovery and Outburst

Swift J1727.8–1613 underwent a bright outburst that was detected on 2023 August 24 (Negoro et al. 2023a; Kennea & Swift Team 2023). MAXI (Matsuoka et al. 2009) monitoring of the source showed it reaching ~ 7 Crab in the 2–20 keV range (see Figure 1(a)), triggering interest and rapid initiation of follow-up multiwavelength campaigns by a number of ground-based and space observatories (Baglio et al. 2023; Miller-Jones et al. 2023; Negoro et al. 2023b; O’Connor et al. 2023; Wang & Bellm 2023; Williams-Baldwin et al. 2023). The beginning of the outburst was observed in the optical wavelengths about 4 days earlier than the first X-ray trigger (Wang & Bellm 2023). Optical spectroscopy taken at the early outburst stages suggest the source is a low-mass X-ray binary (Castro-Tirado et al. 2023), with signatures of an outflow (Mata Sanchez & Muñoz-Darias 2023). On the next and the third day after the X-ray trigger, the X-ray spectral shape was identified to be consistent with the typical hard-state power law with photon index $\Gamma \sim 1.3$ –1.7, as measured by the LEIA imager (Liu et al. 2023) and by the Mikhail Pavlinsky ART-XC telescope (Sunyaev et al. 2023), respectively. Recent NICER observations (taken 25 days after the beginning of the outburst) report substantial contribution of the disk blackbody emission (of temperature $kT_{\text{diskbb}} = 0.6$ keV) and softening of the spectrum ($\Gamma = 2.4$, Bollemeijer et al. 2023). X-ray light curves revealed prominent quasi-periodic oscillations with a slowly increasing (on

timescales of days) central frequency (Bollemeijer et al. 2023; Draghis et al. 2023; Palmer & Parsotan 2023).

The onset of the radio source detected at various frequencies shortly after the X-ray trigger identified the presence of a jet (Bright et al. 2023; Miller-Jones et al. 2023), with a flat spectrum (Vrtilek et al. 2023; S. Trushkin et al. 2023, in preparation) typical to the hard-state sources. A subsequent submillimeter detection and polarization measurements indicate its direction is nearly along the north–south celestial axis ($PA = -4^\circ.1 \pm 3^\circ.5$ on the date closest to IXPE pointing; Vrtilek et al. 2023). The intrinsic optical polarization also seems to be roughly aligned with the north–south direction (Kravtsov et al. 2023). While the mass of the compact object has not been reliably measured yet, all indirect signatures indicate the binary hosts a BH, making it an intriguing target that can be used to probe the accretion geometry.

Figure 1(a) shows the initial stages of the count-rate evolution in Swift J1727.8–1613 as seen by MAXI monitor,⁵⁸ and the typical fast rise profile can be clearly identified. The starting point for the date corresponds to the initial X-ray trigger (which we will refer to as the beginning of the X-ray outburst hereafter). A few days after the beginning of the outburst, the source started to soften (see Figure 1(b)). The source evolution follows the well-known q-track pattern (Homan & Belloni 2005) in the hardness–flux diagram (blue symbols in Figure 1(c)), albeit becoming much brighter than the prominent low-mass X-ray binary MAXI J1820+070 (shown in red) and the prototypical source GX 339–4 (orange). IXPE observed Swift J1727.8–1613 at high, close to current maxima, fluxes, about 15 days after the beginning of the outburst. According to the position in hardness–flux diagram, the source started transition to the soft state and resided in the hard-intermediate state (which we refer to as the hard state hereafter; Figure 1(c)).

⁵⁸ <http://maxi.riken.jp/>

3. Observations and Data Reduction

IXPE is the first satellite mission dedicated to X-ray polarimetry in the 2–8 keV band (Weisskopf et al. 2022). It carries three X-ray telescopes, each made of a mirror module assembly (Ramsey et al. 2022) and a polarization-sensitive gas-pixel detector unit (Baldini et al. 2021; Soffitta et al. 2021), which enable imaging X-ray polarimetry of extended sources and a huge increase of sensitivity for point-like sources. IXPE provides an angular resolution of $\sim 30''$ (half-power diameter). The overlap of the fields of view of the three detector units is circular with a diameter of $9'$; spectral resolution is better than 20% at 6 keV.

IXPE observed Swift J1727.8–1613 from 2023 September 7 19:59:07 UTC to September 8 06:35:12 UTC for a live time of ~ 19 ks (Dovciak et al. 2023a, 2023b). Level 2 data were downloaded from the IXPE archive at the HEASARC⁵⁹ and analyzed with both IXPEOBSSIM version 30.6.2 (Baldini et al. 2022) and HEASOFT/XSPEC version 12.13.1d (Arnaud 1996). IXPE observations of Swift J1727.8–1613 were carried out placing a “gray” filter in front of the detector (Ferrazzoli et al. 2020; Soffitta et al. 2021). The filter was used to reduce (by a factor of ~ 10) the incident flux from a very bright source, especially at low energies, to a level compatible with the dead time of the detector units and with the need to transmit all data within the allocated telemetry. Now different response matrices have to be used for data analysis, which are available both in the IXPEOBSSIM package and in the HEASARC CALDB. Comparing the polarization obtained by the PCUBE algorithm in IXPEOBSSIM and the one from XSPEC, we found that the latter provides more consistent results as it fully takes into account the energy response of the instrument. This is particularly important to correctly describe the low-energy response of the IXPE detectors when the gray filter is used, as its transmission drops steeply at low energies. In the following, we then present the results obtained with XSPEC. Source events were extracted using a circle with $80''$ radius centered on the source. No background subtraction is necessary for sources as bright as Swift J1727.8–1613, since in this case the IXPE background is dominated by scattered source emission, even at large offset (hence, the background itself is negligible and can be ignored; Di Marco et al. 2023).

4. Polarization Results

We fitted Stokes I , Q , and U spectra with XSPEC, using only simple models because of the limited spectral capability of IXPE. We first tested a `polconst*diskbb` model, representing an accretion disk consisting of multiple blackbody components with a constant polarization, using the `gain fit` command in XSPEC to fit the energy scale. We found an unacceptable fit, $\chi^2 = 3509$ for 1329 degrees of freedom (dof), driven by large residuals in the I spectrum. Models for absorption remain unconstrained due to the relatively high IXPE threshold (2 keV) and the use of the gray filter, which strongly reduces the flux from the source at low energies. Then, we used a power-law model assuming constant polarization `polconst*powerlaw`, using `gain fit` command. The data with the best-fit model are shown in Figure 2. The model gives $\chi^2 = 1282$ for 1329 dof. The best-fit power-law index is $\Gamma = 1.80_{-0.01}^{+0.02}$, with the polarization being $\text{PD} = 4.1\% \pm 0.2\%$

at $\text{PA} = 2^\circ 2 \pm 1^\circ 3$. The errors are at 68% confidence level and calculated assuming one interesting parameter with the `steppar` command of XSPEC. The polarization from the source is detected at a $\sim 20\sigma$ confidence level.

We then froze the spectral model to the one found for the 2–8 keV energy band and fitted in the different energy ranges leaving only the polarization model (either `polconst` or `stokesconst`) free to vary. The results are given in Table 1. The PD shows an increasing trend with energy, growing from about 3% in the 2–3 keV band to $\sim 5\%$ above 5 keV. We note that the contribution of the disk with the inner temperature $kT_{\text{diskbb}} \sim 0.5$ keV (Bollemeijer et al. 2023; Draghis et al. 2023) cannot be ruled out in the lower-energy bin and might cause the reduction of PD here. At the same time, the PD at higher energies, which we attribute to the corona, is rather constant. The PA does not show any significant variations with energy. Contours plots of the PD and PA in three energy bands are shown in Figure 3.

We then checked for a possible energy dependence of the polarization by substituting the `polconst` model with `pollin`, which assumes a linear dependence of PD and PA on photon energy. However, we assumed an energy-independent PA (ψ_1 in XSPEC; fixing $\psi_{\text{slope}} = 0$), and allowed the PD to vary with photon energy E (keV) as $\text{PD}(E) = A_1 + A_{\text{slope}}(E - 1)$. We obtained a marginally better fit $\chi^2/\text{dof} = 1277/1328$ with the F -test giving a probability of 3% for a chance improvement. The best-fit parameters are $A_1 = 3.0\% \pm 0.5\%$ and $A_{\text{slope}} = 0.34 \pm 0.13\% \text{ keV}^{-1}$, and $\text{PA} = \psi_1 = 2^\circ 0 \pm 1^\circ 3$.

5. Discussion

The exceptional brightness of the newly discovered source Swift J1727.8–1613 is striking and can be compared to only a few historical BH transients: the low- or intermediate-mass X-ray binaries A0620–00 (Elvis et al. 1975), GRS 1915+105 (Sazonov et al. 1994), V404 Cyg (Życki et al. 1999), V4641 Sgr (Revnivtsev et al. 2002), MAXI J1820+070 (Shidatsu et al. 2018), and 4U 1543–47 (Sánchez-Sierras et al. 2023). The high X-ray fluxes of A0620–00 and MAXI J1820+070 are caused by the proximity of these sources to the observer, and the inferred accretion rates fall in the sub-Eddington category. In these cases, we see the innermost parts of the disk/corona during the hard state. On the other hand, the luminosities of GRS 1915+105, V404 Cyg, V4641 Sgr, and 4U 1543–47 are believed to reach near- and super-Eddington values, and signatures of an optically thick outflow, that can cover the innermost regions, have been detected (Revnivtsev et al. 2002; Motta et al. 2017; Miller et al. 2020; Prabhakar et al. 2023). Analogs to these classes of sources can be found in active galactic nuclei, whose geometry studies are now also enabled by IXPE data. For the hard-spectrum sources where the innermost parts of the accretion disk are visible, the X-ray polarization is found to be in a range of about a few percent (Cyg X-1, Krawczynski et al. 2022; NGC 4151, Gianolli et al. 2023; MCG-05-23-16, Marinucci et al. 2022; Tagliacozzo et al. 2023; IC 4329A, Ingram et al. 2023) and aligned with the jet direction (wherever it is constrained). For the sources where the central engine is obscured, the observed spectrum is dominated by a reflection continuum, and high (PD $> 20\%$) polarization orthogonal to the jet direction (polarization aligned with the obscuring torus) has

⁵⁹ <https://heasarc.gsfc.nasa.gov/docs/ixpe/archive/>

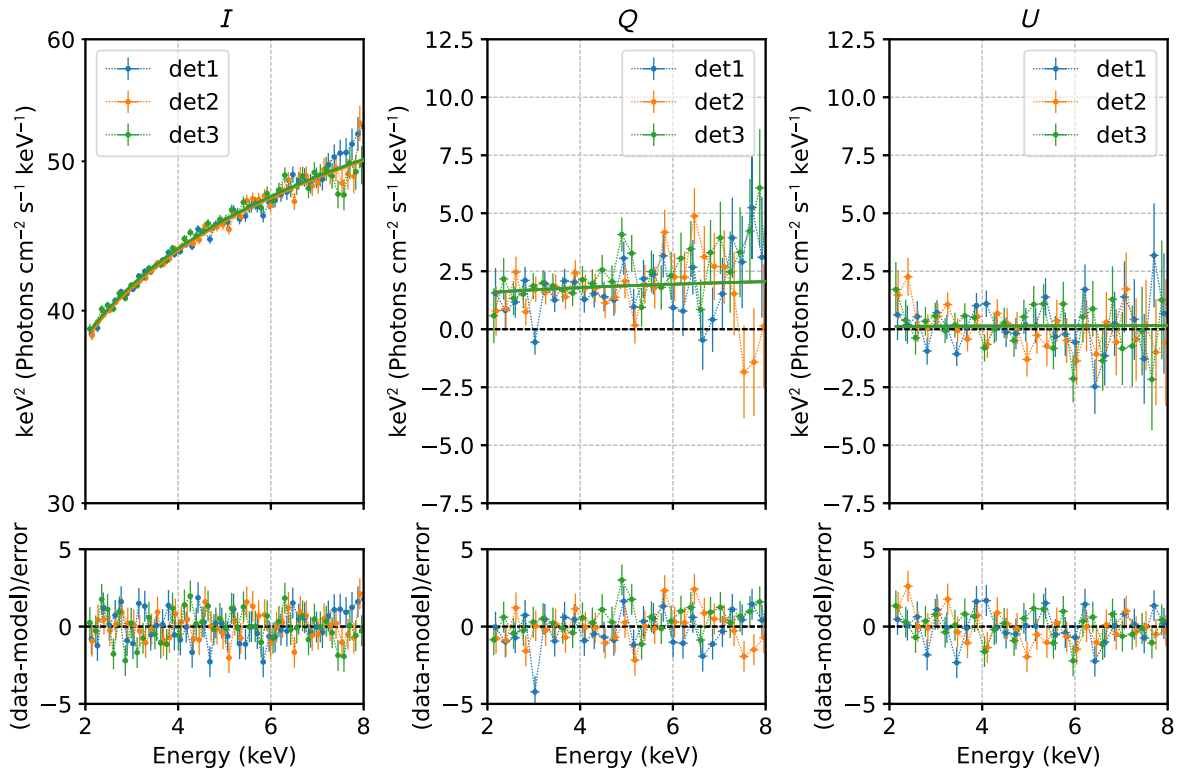


Figure 2. IXPE X-ray spectra of Swift J1727.8–1613. Stokes I , Q , and U spectra are shown in the left, middle, and right panels, respectively. Data from the three IXPE detectors are shown as crosses: det1 (blue), det2 (red), and det3 (green). The best-fit model `polconst*powerlaw` is shown with corresponding lines. The lower subpanels show the fit residuals.

been found (Cyg X-3, Veledina et al. 2023; Circinus galaxy, Ursini et al. 2023).

The relatively low X-ray PD found in Swift J1727.8–1613 (as compared to some other accreting BHs) suggests the innermost parts of the accretion disk are visible, and the geometry is similar to that of Cyg X-1 and Seyfert 1 galaxies. This is supported by the hardness–flux diagram (Figure 1(c)) which indicates that IXPE observed the source at the beginning of the hard-to-soft-state transition. By comparing the flux of Swift J1727.8–1613 at the turning point (at which a source begins softening) with those of other BH X-ray binaries MAXI J1820+070 situated at 3 kpc (Atri et al. 2020) and GX 339–4 at an estimated distance of ~ 10 kpc (Zdziarski et al. 2019), we can estimate that Swift J1727.8–1613 is closer than MAXI J1820+070 by a factor of 2 (i.e., at a distance of about 1.5 kpc).

Relativistic ejections have not yet been observed in the source; hence the direction of the jet is not known from radio images. The submillimeter polarization signal, however, gives a clue as to the jet axis (oriented close to the north–south direction; Vrtilek et al. 2023). It has been found that the intrinsic polarization in the optical, submillimeter, and radio (after correction for Faraday rotation) is aligned with the jet direction in the X-ray binaries during the outburst (Cyg X-3, M. McCollough et al. 2023, in preparation; A. Lange et al. 2023, in preparation; Veledina et al. 2023; XTE J1908+094, Curran et al. 2015; XTE J1550–564, Migliori et al. 2017; MAXI J1820+070, Veledina et al. 2019; and V404 Cyg, Kosenkov et al. 2017). If the jet direction in Swift J1727.8–1613 also aligns with the detected optical and submillimeter polarization, then the X-ray polarization is also aligned with the

jet direction, supporting the analogy to sub-Eddington, rather than super-Eddington sources.

The similarity of the X-ray PA to the submillimeter PA and, by extension, to the position angle of the radio jet is related to the alignment of the jet direction with the BH spin and the jet collimation mechanisms (McKinney et al. 2013; Davis & Tchekhovskoy 2020). If the BH spin is misaligned with the binary orbital axis, the accretion disk/flow becomes warped and/or can experience Lense–Thirring precession (Bardeen & Petterson 1975; Stella & Vietri 1998; Fragile et al. 2007). Precession of the accretion flow may then be visible in multiwavelength light curves as prominent quasi-periodic oscillations (Ingram et al. 2009; Veledina et al. 2013), which are indeed detected in the X-ray timing data on Swift J1727.8–1613 (Draghis et al. 2023; Palmer & Parsotan 2023). We clearly detect two harmonics of these oscillations, at 1.340 ± 0.004 and 2.74 ± 0.04 Hz, in the IXPE flux data (M. Ewing et al. 2023, in preparation). In the case of a substantial misalignment between the orbital and BH spin axes and rapid Lense–Thirring precession of the inner flow, the average (over the precession period) flow axis is aligned with the spin axis. As a consequence, the average X-ray PA is parallel to the BH spin axis. The outer parts of the disk are, on the other hand, expected to be aligned with the orbital plane (e.g., as found in MAXI J1820+070; Poutanen et al. 2022). The alignment of the jet direction with the BH spin in Swift J1727.8–1613 also suggests that the jets are launched from the radii that are either aligned with the BH spin axis or experience rapid precession around it.

The similarity of the detected X-ray PD in Swift J1727.8–1613 and Cyg X-1 may be interpreted as similarity of inclinations of the inner parts of the accretion disk in these

Table 1
Energy Dependence of Polarization Properties

| Parameter | Energy Range (keV) | | | | | | |
|-----------|--------------------|---------------|---------------|----------------|----------------|---------------|---------------|
| | 2–3 | 3–4 | 4–5 | 5–6 | 6–7 | 7–8 | 2–8 |
| Q/I (%) | 3.4 ± 0.5 | 4.2 ± 0.3 | 4.2 ± 0.4 | 4.5 ± 0.5 | 5.1 ± 0.8 | 4.8 ± 1.3 | 4.1 ± 0.2 |
| U/I (%) | 0.9 ± 0.5 | 0.3 ± 0.3 | 0.1 ± 0.4 | 0.0 ± 0.5 | -0.7 ± 0.8 | 0.4 ± 1.3 | 0.3 ± 0.2 |
| PD (%) | 3.5 ± 0.5 | 4.2 ± 0.3 | 4.2 ± 0.4 | 4.5 ± 0.5 | 5.1 ± 0.8 | 4.8 ± 1.3 | 4.1 ± 0.2 |
| PA (deg) | 7.4 ± 3.7 | 2.2 ± 2.3 | 0.7 ± 2.7 | -0.2 ± 3.4 | -3.7 ± 4.2 | 2.3 ± 8.0 | 2.2 ± 1.3 |

Note. Polarization characteristics are obtained from the I , Q , and U Stokes parameters computed with PHA1, PHA1Q, and PHA1U algorithms in xpbins and fitted with polconst*powerlaw model in given energy intervals. The uncertainties are given at the 68.3% (1σ) confidence level for one interesting parameter.

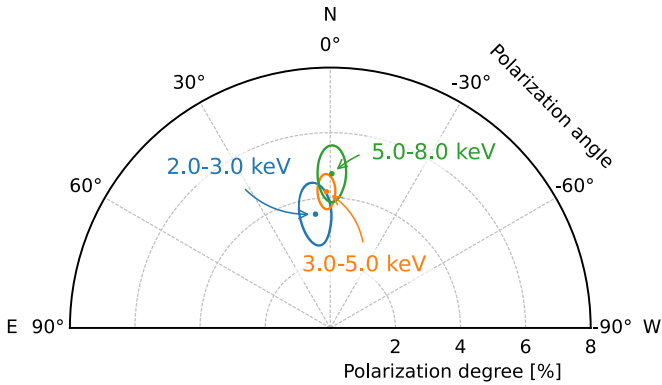


Figure 3. Contour plots of the PD and PA in three energy bands measured with XSPEC at 90% confidence level.

systems, that translates to an intermediate inclination of the source $i \sim 30^\circ$ – 60° . This is further supported by the absence of the X-ray dips. The inclination of the binary orbit can be reliably measured only after the source reaches quiescence (Casares & Jonker 2014), and may help to distinguish between various configurations of the accretion disk and corona. However, basic constraints on the geometry can be made using these first X-ray polarization measurements. While the X-ray PA and its relation to the submillimeter PA suggest that the X-ray corona is extended along the disk (and not along the jet), the high PD $\sim 4\%$, either constant or increasing with energy, argue against spherical and lamppost coronal geometries (Krawczynski et al. 2022; Zhang et al. 2022).

Swift J1727.8–1613 continues to gradually soften, in line with the q-pattern in the hardness–flux diagram (Figure 1(c)). Subsequent observations by IXPE detecting the source in the soft and very high states may enable comparison to the other BH X-ray binaries observed in polarized X-ray light (Dovciak et al. 2023c; Marra et al. 2023; Podgorny et al. 2023; Ratheesh et al. 2023; Rodriguez Cavero et al. 2023; Svoboda et al. 2023), providing independent constraints on the inclination and calibrating the models of accretion disk structure and radiative processes.

6. Summary

We obtained the first X-ray polarization measurement for the bright BH binary Swift J1727.8–1613. We find the time- and energy-averaged $PD = 4.1\% \pm 0.2\%$ and $PA = 2.2 \pm 1.3$ (68% confidence) from XSPEC spectropolarimetric fits. There is no statistically significant dependence of the PA on energy. A model that assumes a linear dependence of PD on energy gives a slight improvement in χ^2 significant at 97% confidence

level and results in a PD increasing with energy by 0.34% per keV.

The evolution of the source in the hardness–flux diagram and the observed spectral slope indicate that the source was in the hard state during IXPE observations, accreting at sub-Eddington rates, so its high X-ray brightness is caused by the source proximity to the Earth. We estimate the distance to the source to be about 1.5 kpc.

The alignment of X-ray, optical, and submillimeter polarization directions indicates that the hot medium producing the X-ray continuum emission is extended in the accretion disk plane (orthogonal to the jet). Our findings support the expectation that the jets are launched orthogonal to the inner parts of the accretion flow. By extension, this means that the direction of the inner parts of the jet in Swift J1727.8–1613 are aligned with the BH spin.

The PD value is comparable to that found in the high-mass BH X-ray binary Cyg X-1, and can, by similarity, constrain the inclination of the innermost parts to be moderate, $i \sim 30^\circ$ – 60° . Also, the trend of PD with energy is inconsistent with the geometry of the spherical or lamppost corona, even if it is outflowing.

Acknowledgments

The Imaging X-ray Polarimetry Explorer (IXPE) is a joint US and Italian mission. The US contribution is supported by the National Aeronautics and Space Administration (NASA) and led and managed by its Marshall Space Flight Center (MSFC), with industry partner Ball Aerospace (contract NNM15AA18C). The Italian contribution is supported by the Italian Space Agency (Agenzia Spaziale Italiana, ASI) through contract ASI-OHBI-2022-13-I.0, agreements ASI-INAF-2022-19-HH.0 and ASI-INFN-2017.13-H0, and its Space Science Data Center (SSDC) with agreements ASI-INAF-2022-14-HH.0 and ASI-INFN 2021-43-HH.0, and by the Istituto Nazionale di Astrofisica (INAF) and the Istituto Nazionale di Fisica Nucleare (INFN) in Italy. This research used data products provided by the IXPE Team (MSFC, SSDC, INAF, and INFN) and distributed with additional software tools by the High-Energy Astrophysics Science Archive Research Center (HEASARC), at NASA Goddard Space Flight Center (GSFC). This research has made use of the MAXI data provided by RIKEN, JAXA, and the MAXI team.

A.V. thanks the Academy of Finland grant 355672 for support. M.D., J.S., J.Pod., and V.Kar. thank GACR project 21-06825X for the support and institutional support from RVO:67985815. A.I. acknowledges support from the Royal Society. H.K. acknowledges support by NASA grants 80NSSC22K1291, 80NSSC23K1041, and 80NSSC20K0329.

V.Kra. acknowledges support from the Finnish Cultural Foundation. The French contribution is supported by the French Space Agency (Centre National d'Etude Spatiale, CNES) and by the High Energy National Programme (PNHE) of the Centre National de la Recherche Scientifique (CNRS). I. L. was supported by the NASA Postdoctoral Program at the Marshall Space Flight Center, administered by Oak Ridge Associated Universities under contract with NASA.












Facilities: IXPE, MAXI.

Software: IXPEOBSSIM (Baldini et al. 2022), XSPEC (Arnaud 1996).

ORCID iDs

Alexandra Veledina  <https://orcid.org/0000-0002-5767-7253>
 Fabio Muleri  <https://orcid.org/0000-0003-3331-3794>
 Michal Dovčiak  <https://orcid.org/0000-0003-0079-1239>
 Juri Poutanen  <https://orcid.org/0000-0002-0983-0049>
 Ajay Ratheesh  <https://orcid.org/0000-0003-0411-4243>
 Fiamma Capitanio  <https://orcid.org/0000-0002-6384-3027>
 Giorgio Matt  <https://orcid.org/0000-0002-2152-0916>
 Paolo Soffitta  <https://orcid.org/0000-0002-7781-4104>
 Allyn F. Tennant  <https://orcid.org/0000-0002-9443-6774>
 Michela Negro  <https://orcid.org/0000-0002-6548-5622>
 Philip Kaaret  <https://orcid.org/0000-0002-3638-0637>
 Enrico Costa  <https://orcid.org/0000-0003-4925-8523>
 Adam Ingram  <https://orcid.org/0000-0002-5311-9078>
 Jiří Svoboda  <https://orcid.org/0000-0003-2931-0742>
 Henric Krawczynski  <https://orcid.org/0000-0002-1084-6507>
 Stefano Bianchi  <https://orcid.org/0000-0002-4622-4240>
 James F. Steiner  <https://orcid.org/0000-0002-5872-6061>
 Javier A. García  <https://orcid.org/0000-0003-3828-2448>
 Vadim Kravtsov  <https://orcid.org/0000-0002-7502-3173>
 Anagha P. Nitindala  <https://orcid.org/0009-0002-7109-0202>
 Melissa Ewing  <https://orcid.org/0000-0001-9349-8271>
 Guglielmo Mastroserio  <https://orcid.org/0000-0003-4216-7936>
 Andrea Marinucci  <https://orcid.org/0000-0002-2055-4946>
 Francesco Ursini  <https://orcid.org/0000-0001-9442-7897>
 Francesco Tombesi  <https://orcid.org/0000-0002-6562-8654>
 Sergey S. Tsygankov  <https://orcid.org/0000-0002-9679-0793>
 Yi-Jung Yang  <https://orcid.org/0000-0001-9108-573X>
 Martin C. Weisskopf  <https://orcid.org/0000-0002-5270-4240>
 Sergei A. Trushkin  <https://orcid.org/0000-0002-7586-5856>
 Elise Egron  <https://orcid.org/0000-0002-1532-4142>
 Maria Noemi Iacolina  <https://orcid.org/0000-0003-4564-3416>
 Maura Pilia  <https://orcid.org/0000-0001-7397-8091>
 Lorenzo Marra  <https://orcid.org/0009-0001-4644-194X>
 Romana Mikušincová  <https://orcid.org/0000-0001-7374-843X>
 Edward Nathan  <https://orcid.org/0000-0002-9633-9193>
 Maxime Parra  <https://orcid.org/0009-0003-8610-853X>
 Pierre-Olivier Petrucci  <https://orcid.org/0000-0001-6061-3480>
 Jakub Podgorný  <https://orcid.org/0000-0001-5418-291X>
 Stefano Tugliani  <https://orcid.org/0000-0002-3318-9036>
 Silvia Zane  <https://orcid.org/0000-0001-5326-880X>
 Wenda Zhang  <https://orcid.org/0000-0003-1702-4917>

Iván Agudo  <https://orcid.org/0000-0002-3777-6182>
 Lucio A. Antonelli  <https://orcid.org/0000-0002-5037-9034>
 Matteo Bachetti  <https://orcid.org/0000-0002-4576-9337>
 Luca Baldini  <https://orcid.org/0000-0002-9785-7726>
 Wayne H. Baumgartner  <https://orcid.org/0000-0002-5106-0463>
 Ronaldo Bellazzini  <https://orcid.org/0000-0002-2469-7063>
 Stephen D. Bongiorno  <https://orcid.org/0000-0002-0901-2097>
 Raffaella Bonino  <https://orcid.org/0000-0002-4264-1215>
 Alessandro Brez  <https://orcid.org/0000-0002-9460-1821>
 Niccolò Bucciantini  <https://orcid.org/0000-0002-8848-1392>
 Simone Castellano  <https://orcid.org/0000-0003-1111-4292>
 Elisabetta Cavazzuti  <https://orcid.org/0000-0001-7150-9638>
 Chien-Ting Chen  <https://orcid.org/0000-0002-4945-5079>
 Stefano Ciprini  <https://orcid.org/0000-0002-0712-2479>
 Alessandra De Rosa  <https://orcid.org/0000-0001-5668-6863>
 Ettore Del Monte  <https://orcid.org/0000-0002-3013-6334>
 Laura Di Gesu  <https://orcid.org/0000-0002-5614-5028>
 Niccolò Di Lalla  <https://orcid.org/0000-0002-7574-1298>
 Alessandro Di Marco  <https://orcid.org/0000-0003-0331-3259>
 Immacolata Donnarumma  <https://orcid.org/0000-0002-4700-4549>
 Victor Doroshenko  <https://orcid.org/0000-0001-8162-1105>
 Steven R. Ehlert  <https://orcid.org/0000-0003-4420-2838>
 Teruaki Enoto  <https://orcid.org/0000-0003-1244-3100>
 Yuri Evangelista  <https://orcid.org/0000-0001-6096-6710>
 Sergio Fabiani  <https://orcid.org/0000-0003-1533-0283>
 Riccardo Ferrazzoli  <https://orcid.org/0000-0003-1074-8605>
 Shuichi Gunji  <https://orcid.org/0000-0002-5881-2445>
 Jeremy Heyl  <https://orcid.org/0000-0001-9739-367X>
 Wataru Iwakiri  <https://orcid.org/0000-0002-0207-9010>
 Svetlana G. Jorstad  <https://orcid.org/0000-0001-6158-1708>
 Vladimir Karas  <https://orcid.org/0000-0002-5760-0459>
 Fabian Kislak  <https://orcid.org/0000-0001-7477-0380>
 Jeffery J. Kolodziejczak  <https://orcid.org/0000-0002-0110-6136>
 Fabio La Monaca  <https://orcid.org/0000-0001-8916-4156>
 Luca Latronico  <https://orcid.org/0000-0002-0984-1856>
 Ioannis Liodakis  <https://orcid.org/0000-0001-9200-4006>
 Simone Maldera  <https://orcid.org/0000-0002-0698-4421>
 Alberto Manfreda  <https://orcid.org/0000-0002-0998-4953>
 Frédéric Marin  <https://orcid.org/0000-0003-4952-0835>
 Alan P. Marscher  <https://orcid.org/0000-0001-7396-3332>
 Herman L. Marshall  <https://orcid.org/0000-0002-6492-1293>
 Francesco Massaro  <https://orcid.org/0000-0002-1704-9850>
 Tsunefumi Mizuno  <https://orcid.org/0000-0001-7263-0296>
 Chi-Yung Ng  <https://orcid.org/0000-0002-5847-2612>
 Stephen L. O'Dell  <https://orcid.org/0000-0002-1868-8056>
 Nicola Omodei  <https://orcid.org/0000-0002-5448-7577>
 Chiara Oppedisano  <https://orcid.org/0000-0001-6194-4601>
 Alessandro Papitto  <https://orcid.org/0000-0001-6289-7413>
 George G. Pavlov  <https://orcid.org/0000-0002-7481-5259>
 Abel L. Peirson  <https://orcid.org/0000-0001-6292-1911>
 Matteo Perri  <https://orcid.org/0000-0003-3613-4409>
 Melissa Pesce-Rollins  <https://orcid.org/0000-0003-1790-8018>
 Andrea Possenti  <https://orcid.org/0000-0001-5902-3731>
 Simonetta Puccetti  <https://orcid.org/0000-0002-2734-7835>
 Brian D. Ramsey  <https://orcid.org/0000-0003-1548-1524>
 John Rankin  <https://orcid.org/0000-0002-9774-0560>
 Oliver J. Roberts  <https://orcid.org/0000-0002-7150-9061>
 Roger W. Romani  <https://orcid.org/0000-0001-6711-3286>
 Carmelo Sgrò  <https://orcid.org/0000-0001-5676-6214>
 Patrick Slane  <https://orcid.org/0000-0002-6986-6756>

Gloria Spandre  <https://orcid.org/0000-0003-0802-3453>
 Douglas A. Swartz  <https://orcid.org/0000-0002-2954-4461>
 Toru Tamagawa  <https://orcid.org/0000-0002-8801-6263>
 Fabrizio Tavecchio  <https://orcid.org/0000-0003-0256-0995>
 Roberto Taverna  <https://orcid.org/0000-0002-1768-618X>
 Nicholas E. Thomas  <https://orcid.org/0000-0003-0411-4606>
 Alessio Trois  <https://orcid.org/0000-0002-3180-6002>
 Roberto Turolla  <https://orcid.org/0000-0003-3977-8760>
 Jacco Vink  <https://orcid.org/0000-0002-4708-4219>
 Kinwah Wu  <https://orcid.org/0000-0002-7568-8765>
 Fei Xie  <https://orcid.org/0000-0002-0105-5826>

References

- Arnaud, K. A. 1996, in ASP Conf. Ser. 101, *Astronomical Data Analysis Software and Systems V*, ed. G. H. Jacoby & J. Barnes (San Francisco: ASP), 17
- Atri, P., Miller-Jones, J. C. A., Bahramian, A., et al. 2020, *MNRAS*, 493, L81
- Baglio, M. C., Casella, P., Testa, V., et al. 2023, *ATel*, 16225, 1
- Baldini, L., Barbanera, M., Bellazzini, R., et al. 2021, *APh*, 133, 102628
- Baldini, L., Bucciantini, N., Di Lalla, N., et al. 2022, *SoftX*, 19, 101194
- Bambi, C., Brenneman, L. W., Dauser, T., et al. 2021, *SSRv*, 217, 65
- Bardeen, J. M., & Petterson, J. A. 1975, *ApJL*, 195, L65
- Belloni, T. M. 2010, in *The Jet Paradigm*, ed. T. Belloni (Berlin: Springer Verlag), 53
- Bollemeijer, N., Uttley, P., Buisson, D., et al. 2023, *ATel*, 16247, 1
- Bright, J., Farah, W., Fender, R., et al. 2023, *ATel*, 16228, 1
- Casares, J., & Jonker, P. G. 2014, *SSRv*, 183, 223
- Castro-Tirado, A. J., Sanchez-Ramirez, R., Caballero-Garcia, M. D., et al. 2023, *ATel*, 16208, 1
- Curran, P. A., Miller-Jones, J. C. A., Rushton, A. P., et al. 2015, *MNRAS*, 451, 3975
- Davis, S. W., & Tchekhovskoy, A. 2020, *ARA&A*, 58, 407
- Dexter, J., & Quataert, E. 2012, *MNRAS*, 426, L71
- Di Marco, A., Soffitta, P., Costa, E., et al. 2023, *AJ*, 165, 143
- Done, C., Gierliński, M., & Kubota, A. 2007, *A&ARv*, 15, 1
- Dovciak, M., Ratheesh, A., Tennant, A., & Matt, G. 2023a, *ATel*, 16237, 1
- Dovciak, M., Ratheesh, A., Tennant, A., & Matt, G. 2023b, *ATel*, 16242, 1
- Dovciak, M., Steiner, J. F., Krawczynski, H., & Svoboda, J. 2023c, *ATel*, 16084, 1
- Draghis, P. A., Miller, J. M., Homan, J., et al. 2023, *ATel*, 16219, 1
- Elvis, M., Page, C. G., Pounds, K. A., Ricketts, M. J., & Turner, M. J. L. 1975, *Natur*, 257, 656
- Ferrazzoli, R., Muleri, F., Lefevre, C., et al. 2020, *JATIS*, 6, 048002
- Fragile, P. C., Blaes, O. M., Anninos, P., & Salmonson, J. D. 2007, *ApJ*, 668, 417
- Gianolli, V. E., Kim, D. E., Bianchi, S., et al. 2023, *MNRAS*, 523, 4468
- Homan, J., & Belloni, T. 2005, *Ap&SS*, 300, 107
- Ingram, A., Done, C., & Fragile, P. C. 2009, *MNRAS*, 397, L101
- Ingram, A., Ewing, M., Marinucci, A., et al. 2023, *MNRAS*, 525, 5437
- Jiang, Y.-F., Stone, J. M., & Davis, S. W. 2013, *ApJ*, 778, 65
- Kennea, J. A. & Swift Team 2023, *GCN*, 34540, 1
- Kosenkov, I. A., Berdyugin, A. V., Piirola, V., et al. 2017, *MNRAS*, 468, 4362
- Kravtsov, V., Nitindala, A. P., Veledina, A., et al. 2023, *ATel*, 16245, 1
- Krawczynski, H., Muleri, F., Dovciak, M., et al. 2022, *Sci*, 378, 650
- Liu, H. Y., Li, D. Y., Pan, H. W., et al. 2023, *ATel*, 16210, 1
- Marinucci, A., Muleri, F., Dovciak, M., et al. 2022, *MNRAS*, 516, 5907
- Marra, L., Brigitte, M., Rodriguez Caverro, N., et al. 2023, *A&A*, submitted, arXiv:2310.11125
- Mata Sanchez, D., & Muñoz-Darias, T. 2023, *ATel*, 16216, 1
- Matsuoka, M., Kawasaki, K., Ueno, S., et al. 2009, *PASJ*, 61, 999
- McKinney, J. C., Tchekhovskoy, A., & Blandford, R. D. 2013, *Sci*, 339, 49
- Migliori, G., Corbel, S., Tomsick, J. A., et al. 2017, *MNRAS*, 472, 141
- Miller, J. M., Zoghbi, A., Raymond, J., et al. 2020, *ApJ*, 904, 30
- Miller-Jones, J. C. A., Bahramian, A., Orosz, J. A., et al. 2021, *Sci*, 371, 1046
- Miller-Jones, J. C. A., Sivakoff, G. R., Bahramian, A., & Russell, T. D. 2023, *ATel*, 16211, 1
- Motta, S. E., Kajava, J. J. E., Sánchez-Fernández, C., et al. 2017, *MNRAS*, 471, 1797
- Negoro, H., Serino, M., Nakajima, M., et al. 2023a, *GCN*, 34544, 1
- Negoro, H., Serino, M., Nakajima, M., et al. 2023b, *ATel*, 16205, 1
- Novikov, I. D., & Thorne, K. S. 1973, in *Black Holes (Les Astres Occlus)*, ed. C. DeWitt & B. DeWitt (London: Gordon and Breach), 343
- O'Connor, B., Hare, J., Younes, G., et al. 2023, *ATel*, 16207, 1
- Page, D. N., & Thorne, K. S. 1974, *ApJ*, 191, 499
- Palmer, D. M., & Parsotan, T. M. 2023, *ATel*, 16215, 1
- Podgorny, J., Marra, L., Muleri, F., et al. 2023, *MNRAS*, 526, 5964
- Poutanen, J., Veledina, A., & Beloborodov, A. M. 2023, *ApJL*, 949, L10
- Poutanen, J., Veledina, A., Berdyugin, A. V., et al. 2022, *Sci*, 375, 874
- Poutanen, J., Veledina, A., & Zdziarski, A. A. 2018, *A&A*, 614, A79
- Prabhakar, G., Mandal, S., Bhuvana, G. R., & Nandi, A. 2023, *MNRAS*, 520, 4889
- Ramsey, B. D., Bongiorno, S. D., Kolodziejczak, J. J., et al. 2022, *JATIS*, 8, 024003
- Ratheesh, A., Dovciak, M., Krawczynski, H., et al. 2023, *ApJ*, submitted, arXiv:2304.12752
- Remillard, R. A., & McClintock, J. E. 2006, *ARA&A*, 44, 49
- Revnitsev, M., Gilfanov, M., Churazov, E., & Sunyaev, R. 2002, *A&A*, 391, 1013
- Rodriguez Caverro, N., Marra, L., Krawczynski, H., et al. 2023, *ApJL*, in press, arXiv:2305.10630
- Sánchez-Sierras, J., Muñoz-Darias, T., Casares, J., et al. 2023, *A&A*, 673, A104
- Sazonov, S. Y., Syunyaev, R. A., Lapshov, I. Y., et al. 1994, *AstL*, 20, 787
- Shakura, N. I., & Sunyaev, R. A. 1973, *A&A*, 24, 337
- Shidatsu, M., Nakahira, S., Yamada, S., et al. 2018, *ApJ*, 868, 54
- Soffitta, P., Baldini, L., Bellazzini, R., et al. 2021, *AJ*, 162, 208
- Stella, L., & Vietri, M. 1998, *ApJL*, 492, L59
- Sunyaev, R. A., Mereminskiy, I. A., Molkov, S. V., et al. 2023, *ATel*, 16217, 1
- Svoboda, J., Dovciak, M., Steiner, J. F., et al. 2023, *ApJ*, in press, arXiv:2309.10813
- Tagliacozzo, D., Marinucci, A., Ursini, F., et al. 2023, *MNRAS*, 525, 4735
- Tananbaum, H., Gursky, H., Kellogg, E., Giacconi, R., & Jones, C. 1972, *ApJL*, 177, L5
- Ursini, F., Marinucci, A., Matt, G., et al. 2023, *MNRAS*, 519, 50
- Veledina, A., Berdyugin, A. V., Kosenkov, I. A., et al. 2019, *A&A*, 623, A75
- Veledina, A., Muleri, F., Poutanen, J., et al. 2023, arXiv:2303.01174
- Veledina, A., Poutanen, J., & Ingram, A. 2013, *ApJ*, 778, 165
- Vrtilek, S. D., Gurwell, M., McCollough, M., & Rao, R. 2023, *ATel*, 16230, 1
- Wang, Y. D., & Bellm, E. C. 2023, *ATel*, 16209, 1
- Weisskopf, M. C., Soffitta, P., Baldini, L., et al. 2022, *JATIS*, 8, 026002
- Williams-Baldwin, D., Motta, S., Rhodes, L., et al. 2023, *ATel*, 16231, 1
- Zdziarski, A. A., & Gierliński, M. 2004, *PThPS*, 155, 99
- Zdziarski, A. A., Ziółkowski, J., & Mikołajewska, J. 2019, *MNRAS*, 488, 1026
- Zhang, W., Dovciak, M., Bursa, M., et al. 2022, *MNRAS*, 515, 2882
- Życki, P. T., Done, C., & Smith, D. A. 1999, *MNRAS*, 309, 561